IEEE Access
Multidisciplinary | Rapid Review | Open Access Journal

Received November 15, 2021, accepted November 29, 2021, date of publication December 1, 2021,
date of current version December 9, 2021.

Digital Object Identifier 10.1109/ACCESS.2021.3132009

Performance Analysis of UAV Assisted Mobile Communications in THz Channel

SARA FARRAG[1], ENGY MAHER[1], AHMED EL-MAHDY[1], AND FALKO DRESSLER[2], (Fellow, IEEE)
[1]Faculty of Information Engineering and Technology, German University in Cairo, Cairo 16482, Egypt
[2]Telecommunication Networks Group, TU Berlin, 10623 Berlin, Germany

Corresponding author: Sara Farrag (sarah.farrag@guc.edu.eg)

This work was supported by the DAAD through the German Federal Ministry of Education and Research, in Co-Operation Between the Department of Telecommunications Systems at TU Berlin and the German University in Cairo.

ABSTRACT The huge available bandwidth in Terahertz (THz) frequency band is recently contemplated to achieve high data rate wireless communications. Consequently, THz communications are attractive candidates to fulfill the continuous ever–increasing requirements of future wireless networks. Numerous beyond 5G applications are highly considered for those systems such as high capacity backhaul, enhanced hotspot booths as well as short–range device–to–device (D2D) communications. Wireless communications systems that deploy unmanned aerial vehicles (UAVs) promise to achieve cost–effective wireless connectivity for devices without any need to pay for infrastructure coverage. When compared to terrestrial communications, wireless systems with UAVs are generally faster and more flexible to deploy or reconfigure. In addition, systems deploying UAVs are likely to have much better communication channels due to their high mobility capabilities. Accordingly, the presence of short–range line–of–sight (LOS) links prevail. In this paper, we consider a single–cell cellular network with a UAV deployed as a decode-and-forward (DF) relay in the full-duplex (FD) mode in order to assist a base station (BS) and extend its coverage over THz channel. A joint power allocation and trajectory optimization scheme that minimizes the outage probability of the link between the BS and a mobile device (MD) is derived in the presence of the interference of the D2D devices that share the same THz frequency band. Furthermore, the optimum powers of the MD and the UAV that maximize the achievable rate at the BS are obtained. The performance of the proposed schemes is compared with the fixed power allocation schemes which distribute the power equally among users. Numerical results show that the outage probability and the achievable rate at the BS using the proposed schemes are remarkably superior compared to the fixed power allocation schemes.

INDEX TERMS Wireless communications, UAV, terahertz, D2D, DF relay, uplink, power optimization, outage probability.

I. INTRODUCTION

Over the last few years, data traffic over cellular networks has experienced a radical growth, mainly due to the explosion of smartphones, tablets, and laptops. This increase in data traffic on cellular networks has resulted in an ever–increasing need for offloading traffic for optimum performance of both voice and data services. The remarkable expansion of wireless data traffic has advocated the investigation of gap regions in the radio spectrum to meet the users' demands in the radio spectrum to satisfy users' escalating requirements and promise for the exploitation of high capacity and massive connectivity [1], [2].

Examining the spectrum below 6 GHz, it is found congested and in excessive use by existing mobile networks, WiFi, broadcasting and satellite communications. Furthermore, for millimeter wave (mmWave) communication systems, they can only support data rates in the order of 10 Gbps within one meter, which is still two orders of magnitudes below the needed requirements [3]. Nevertheless, THz band communication is a key wireless technology to satisfy those objectives by solving the spectrum scarcity problems and capacity limitations of current wireless systems. With deploying communications systems in the THz band,

The associate editor coordinating the review of this manuscript and approving it for publication was Bong Jun David Choi.

terabit–per–second (Tbps) links are predicted to become a reality within the few upcoming years. Hence, on its turn, THz is capable of enabling numerous long– awaited applications in various aspects with its promising high throughput and low latency. It is noteworthy that THz band is also an auspicious candidate to offload traffic from cellular band and introduce better service for short–range communicating nodes [4]. Consequently, the THz frequency band (0.1-10 THz) has recently received noticeable attention within the global community because of its capabilities to offer seemless data transfer, wide bandwidth that theoretically can reach up to some THz, potential capacity in terabit per second, latency in the order of microseconds and ultra–fast download capabilities. All these qualifications give this particular frequency range superiority in comparison to optical frequencies [5]. Additionally, the THz waves are more suitable candidates for uplink communication. In other words, they allow non–line–of–sight (NLOS) propagation and function as reliable substitutes in troublesome climate conditions such as dust, turbulence rain and fog. Moreover, the THz frequency band is not affected by surrounding noise caused by optical sources and it is not correlated with any safety limits or health problems [6]. Compared to wireless optical communications, THz communication systems are not sensitive to atmospheric effects in outdoor wireless communications. For indoor wireless communications, the THz frequency band can track the beam much easier than the optical frequency band [7]. In addition, with such an available bandwidth, THz communication systems are capable of offering much more bandwidth than traditional microwave communication systems since transmission rates in the widely utilized microwave frequency bands are restricted by the limited allocated spectra that is typically a few 100 MHz [8]. This definitely makes the THz frequency band more superior to the microwave band as well as more suitable for the ever–increasing data traffic in future wireless communications [7].

However, the excessive available bandwidth advantage of the THz band communications comes always at the expense of great propagation loss [9]. Generally, this substantial loss is arisen as the electromagnetic wave propagates through the medium as well as the absorption loss caused by the molecular absorption of the water vapor molecules in the atmosphere [10], [11]. Those highly demanding properties that characterize only THz frequency range are expected to revolutionize the telecommunications landscape and change the route through which people communicate, share and use information [12]–[14].

The use of flying platforms such as UAVs or drones is rapidly enlarging. Thanks to their flexibility and high mobility, UAVs are vital in numerous potential applications in wireless systems such as aerial base stations to enhance coverage, reliability, energy efficiency and capacity of wireless networks [15]–[18]. UAV relaying is one of those various UAV applications in which the UAV is deployed in the network to attain wireless connectivity between a couple of nodes in the case of no existing direct communication link between them. This particular application is considered an efficacious technique to increase throughput, improve reliability as well as to extend the BS coverage [10], [19]. The high mobility of the UAV relay can improve the communication performance by dynamically adjusting the UAV location that best suits the surroundings. Moreover, combining THz and low–altitude UAV is characterized by a higher chance of LOS with the ground user equipments (UEs), which in turn makes the deployment of UAVs to support THz communications a very auspicious solution [20]. In fact, deploying D2D communication in cellular networks allows mobile devices to communicate directly with each other under the control of the BS to cope with the tremendous pressure on cellular networks with limited spectrum resources. It is also worth mentioning that the deploying of THz band D2D communication makes the computing, uploading and downloading between two close UEs near–real time [21]. There are multiple research works from the literature that consider D2D communications in THz frequency band [22]–[24]. Although this can help in uploading the main cellular network, more complex interference is observed in D2D heterogeneous networks due to reusing the same resources. In fact, D2D communication has been intensely inspected and deeply studied in the RF as well as mmWave bands. In addition, there are various difficulties arisen when deploying it in THz band [25].

II. RELATED WORK

In [17], the authors studied three typical application scenarios for mmWave–UAV communications, communication terminal, access point and backbone point. Numerous key enabling techniques for UAV communications are presented including beam tracking, multi–beam forming, FD relaying techniques as well as transmitter\receiver beam alignment. In [18], 3D beamforming for mmWave UAV communications with a phased uniform planar array is investigated. In their work, the authors proved that their approach is capable of achieving flexible beam coverage for all types of target area. Moreover, it was proven that the beamforming gain is mostly concentrated in the target coverage area. The authors in [26] employed a FD–UAV relay in order to increase the communications capacity of the mmWave networks. In their design, large antenna arrays are equipped at the source node (SN), the destination node (DN) and the FD–UAV relay in order to solve the problem of high pathloss of mmWave channels and help in mitigating the self–interference at the FD–relay. Accordingly, the authors formulate a problem for maximizing the achievable rate from the SN to the DN, where they target at jointly optimizing the UAV position, analog beam forming and power control.

It is noteworthy that the most significant attribute of THz communications exists in its capability to facilitate mobile communications at both the access level and the device level in D2D and drone– to– drone communications [27]. There are handful papers deploying UAV communication over the THz channel [28]–[30]. The authors in [28] analyzed the

orientation and position estimation capabilities of the THz multiple input multiple output (MIMO)–orthogonal frequency division multiplexing (OFDM) link between two UAVs based on both the position and the orientation error bound. Their simulations concluded that millimeter–level positioning accuracy that is needed for distributed sensing is achievable in case the separation distance between the transmitter and receiver is sufficiency small. In addition, their simulations revealed that increasing the bandwidth beyond a specific point does not lead to any notable increase in positioning accuracy. The authors in [29] investigated the challenges in enabling high data rate and low latency infrastructure–less wireless UAVs networking in mmWave and THz–band communications. They mainly studied the effects of mobile uncertainties on mmWave and THz bands.

From the above discussion, it is noted that researchers do not focus on evaluating the outage probability of the model that combines THz and D2D technologies with a mobile FD–UAV operating in the same frequency band. Then, the contributions of the paper are as follows:

1) The total outage probability of the communication link from MD to UAV and from UAV to BS is derived in THz channel in the presence of the UAV self–interference and the interference from D2D devices that utilize exactly the same frequency resources.
2) The joint power allocation and trajectory optimization scheme which minimizes the outage probability of the link between the BS and an MD is derived in the presence of the interference of the D2D devices.
3) In addition, the rate maximization optimization problem at the BS is derived and the optimum powers of the MD and the UAV that maximize the SINR at the BS are also obtained.

It is worth mentioning that this work is an extension of our work published in [30], where the UAV position here is no longer fixed to make the best use of the UAV mobility and flexibility. In other words, a dynamic position of the UAV is now considered to generalize the model submitted in [30].

III. SYSTEM AND CHANNEL MODEL

In this section, the system model and the channel model are provided.

A. SYSTEM MODEL

We consider an individual cell cellular network as shown in Fig. 1 that involves one MD, one UAV, one BS and M D2D device pairs that coexist and share the same frequency resources with the MD and the UAV. The direct link between the MD and the BS is not achievable due to high loss resulting from lengthy distances travelled or the presence of obstacles such as mountains, trees, sky–scrapers. With the help of a UAV employed between the MD and the BS to operate as a DF relay, the communication link between the MD and the BS is promoted and LOS is achieved between the MD and

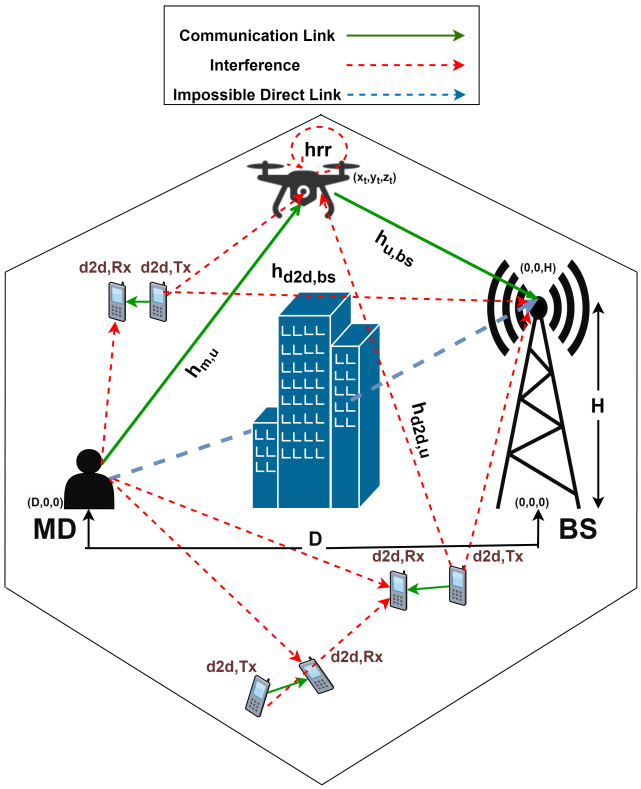

FIGURE 1. Scenario under consideration where a UAV is serving as a DF-FD relay that assists the communication link between the MD and the BS with some D2D pairs coexist.

the UAV as well as between the UAV and the BS. The UAV is anticipated to operate in FD mode to increase the data rate. Therefore, the UAV is equipped with a couple of antennas (one transmit antenna and one receive antenna), meanwhile the other devices in the network are equipped with a single antenna.

The interference from the UAV–transmit antenna is remarkable and cannot be neglected even with the deploying of modern self–interference cancellation techniques.

Without loss of generality, consider an MD is located at $(D, 0, 0)$ in a Cartesian coordinate system, where D is the distance from the MD to the BS as shown in Fig. 1. The BS is located at $(0, 0, H)$, where H is its height as indicated. The UAV's location at time t is assumed to be (x_t, y_t, z_t). Therefore, the distance from the MD to the UAV (i.e. $D_{M,U}$) and the distance from the UAV to the BS (i.e. $D_{U,BS}$) at time t can be calculated from Fig. 2 and are given respectively by:

$$D_{M,U} = \sqrt{(x_t - D)^2 + y_t^2 + z_t^2}, \tag{1}$$

$$D_{U,BS} = \sqrt{x_t^2 + y_t^2 + (z_t - H)^2}. \tag{2}$$

Let M represents the number of D2D pairs. The transmit powers of the MD, the UAV, the i_{th} D2D transmitter and the self-interference power at the UAV are denoted as: P_M, P_U, P_{d2d_i} and P_{rr} respectively. The communication channels between the nodes in the network are assumed to be

THz channels. All the channels between the nodes are assumed to be known or perfectly estimated. The description of this channel is provided in the next subsection.

B. CHANNEL MODEL

In the following, we introduce the THz channel model that was developed using THz wave atmospheric transmission attenuation model as well as water vapour absorption. The LOS THz channel gain can be formulated as [31]–[33]:

$$h = \sqrt{\frac{1}{PL(f,d)}}, \tag{3}$$

where $PL(f,d)$ is the pathloss that frequency f suffers when traveling a distance d.

Particularly, $PL(f,d)$ involves spreading loss $L_{sl}(f,d)$ and molecular absorption $L_{mal}(f,d)$ that must be highly considered in the THz band. The spreading loss $L_{sl}(f,d)$ is resulting from the expansion of the electromagnetic wave as it propagates through different mediums. However, the molecular absorption $L_{mal}(f,d)$ is a result of the collisions generated by atmospheric gas or water molecules. Extensive research on the effect of atmospheric attenuation was conducted in [31], [32]. The channel coefficient h follows zero–mean complex Gaussian distribution with variance that models free space path as well as molecular absorption gain. From [32] (Eqn. (2), (3) and (5)), the pathloss at frequency f after propagating a distance d is related to the variance of the THz channel and is expressed as:

$$\begin{aligned} PL(f,d) &= \frac{1}{\sigma^2} = L_{sl}(f,d)L_{mal}(f,d), \\ &= \frac{1}{G_{Tx}G_{Rx}}\left(\frac{4\pi fd}{c}\right)^2 e^{k(f)d}, \end{aligned} \tag{4}$$

where σ^2 is the variance of the THz channel with zero mean and hence, $h \sim CN(0,\sigma^2)$. G_{Tx} and G_{Rx} are the transmitter and the receiver antenna gains, c is the speed of light in free space and $k(f)$ is the frequency dependent medium absorption coefficient that is provided in [34].

IV. MATHEMATICAL FORMULATION

A. SINR EVALUATIONS

The received signal at the UAV can be expressed as

$$\begin{aligned} Y_U = &\underbrace{\sqrt{P_M}h_{M,U}X_M}_{\text{transmitting signal of MD}} + \underbrace{\gamma_r\sqrt{P_{rr}}h_{rr}X_U}_{\text{self-interference signal}} \\ &+ \underbrace{\sum_{i=1}^{M}\sqrt{P_{d2d_i}}h_{d2d_i,U}X_{d2d_i}}_{\text{interference signal from D2D transmitting devices}} + \underbrace{n_U}_{\text{noise}}, \end{aligned} \tag{5}$$

where P_M is the transmitting power of the MD, $h_{M,U}$ is the channel gain from the MD to the UAV, X_M is the transmitting signal of the MD and has unit energy, γ_r is the UAV self-interference factor, P_{rr} is the self-interference power of the UAV, h_{rr} is the self-interference channel experienced at the UAV, X_U is the transmitting signal of the UAV and has unit energy, P_{d2d_i} is the transmitting power of the i_{th} D2D device, $h_{d2d_i,U}$ is the channel gain sensed at the UAV from the transmitting device of the i_{th} D2D pair, X_{d2d_i} is the transmitting signal of the D2D transmitting device of the i^{th} D2D pair and has unit energy, n_U denotes the additive white Gaussian noise (AWGN) at the UAV which has zero mean and variance N_o.

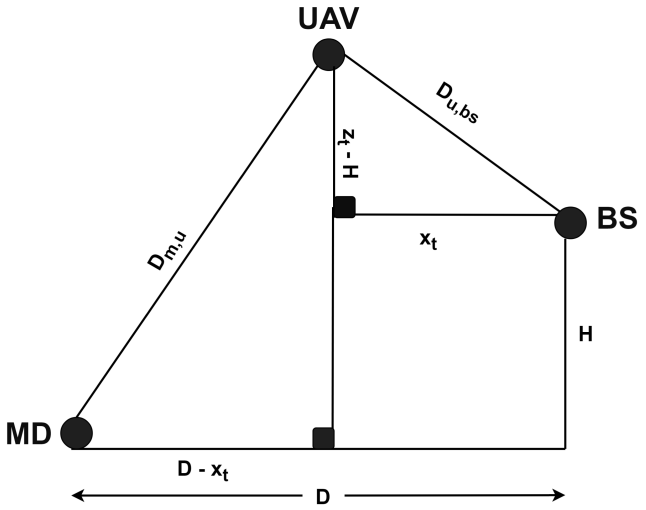

FIGURE 2. Abstract Model of the Communication Link between the MD and the BS at any time *t*.

The received signal at the BS can be written as:

$$\begin{aligned} Y_{BS} = &\underbrace{\sqrt{P_U}h_{U,BS}X_U}_{\text{transmitting signal of UAV}} + \underbrace{\sum_{i=1}^{M}\sqrt{P_{d2d_i}}h_{d2d_i,BS}X_{d2d_i}}_{\text{interference signal from D2D devices}} \\ &+ \underbrace{n_{BS}}_{\text{noise}}, \end{aligned} \tag{6}$$

where P_U is the transmitting power of the UAV, $h_{U,BS}$ is the channel gain from the UAV to the BS, $h_{d2d_i,BS}$ is the channel gain sensed at the BS from the transmitting device of the i_{th} D2D pair and n_{BS} denotes the AWGN at the BS.

Assuming all D2D devices have the same transmitting power P_{d2d}, then from (5) and (6), the signal to-interference-noise-ratio (SINR) at the UAV and the SINR at the BS are given respectively as:

$$\gamma_U = \frac{P_M||h_{M,U}||^2}{P_{d2d}\sum_{i=1}^{M}||h_{d2d_i,U}||^2 + \gamma_r{}^2P_{rr}||h_{rr}||^2 + N_o}, \tag{7}$$

$$\gamma_{BS} = \frac{P_U||h_{U,BS}||^2}{P_{d2d}\sum_{i=1}^{M}||h_{d2d_i,BS}||^2 + N_o}. \tag{8}$$

The received signal of the i_{th} D2D receiving device is expressed as:

$$Y_{d2d_i} = \underbrace{\sqrt{P_{d2d}}h_{d2d_{Tx_i},d2d_{Rx_i}}X_{d2d_i}}_{\text{transmitting signal of D2D i}} + \underbrace{\sqrt{P_M}h_{M,d2d_i}X_M}_{\text{interference signal from MD}}$$

$$+ \underbrace{\sqrt{P_U} h_{U,d2d_i} X_U}_{\text{interference signal from UAV}} + \underbrace{\sqrt{P_{d2d}} \sum_{j=1, j\neq i}^{M} h_{d2d_{Tx_j}, d2d_{Rx_j}} X_{d2d_j}}_{\text{interference signal from other D2D transmitters}} + \underbrace{n_{d2d_i}}_{\text{noise}}, \tag{9}$$

where $h_{d2d_{Tx_i}, d2d_{Rx_i}}$ is the channel gain from the i_{th} transmitting D2D device to the i_{th} receiving D2D device, $h_{M,d2d_i}$ is the channel gain from the MD to the i_{th} D2D receiving device, $h_{U,d2d_i}$ is the channel gain from the UAV to the i_{th} D2D receiving device and n_{d2d_i} denotes the noise at the i_{th} D2D receiving device which has Gaussian distribution (AWGN) with zero mean and variance N_o.

Therefore, from (9), the SINR of the i_{th} D2D receiving device is given by:

$$\gamma_{d2d_i} = P_{d2d} ||h_{d2d_{Tx_i}, d2d_{Rx_i}}||^2 \times \Big[(P_M ||h_{M,d2d_i}||^2 + P_U ||h_{U,d2d_i}||^2 + P_{d2d} \sum_{j=1, j\neq i}^{M} ||h_{d2d_{Tx_j}, d2d_{Rx_j}}||^2 + N_o) \Big]^{-1}. \tag{10}$$

B. OUTAGE PROBABILITY EXPRESSION

The outage probability of the communication link between the MD and the BS is previously derived in detail in our previous work [30] and expressed as:

$$P_{out} = 1 - \Big\{ \exp\Big[- \frac{\beta_{th} (4\pi f)^2}{2C^2 G_U} (Y \frac{P_{d2d} \sum_{i=1}^{M} ||h_{d2d_i,U}||^2 + X}{P_M}) \Big] \times \exp\Big[- \frac{\beta_{th} (4\pi f)^2}{2C^2 G_U} (Z \frac{P_{d2d} \sum_{i=1}^{M} ||h_{d2d_i,BS}||^2 + N_o}{P_U}) \Big] \Big\}. \tag{11}$$

where

$$X = N_o + {\gamma_r}^2 P_{rr} ||h_r||^2, \tag{12}$$

$$Y = \frac{D_{M,U}^2 e^{k(f) D_{M,U}}}{G_M}, \tag{13}$$

$$Z = \frac{D_{U,BS}^2 e^{k(f) D_{U,BS}}}{G_U}. \tag{14}$$

In the following, the optimum powers of the MD and the UAV that minimize the outage probability given in (11) will be derived. Moreover, the optimum trajectory of the UAV that minimizes the outage probability is also obtained.

V. JOINT POWER ALLOCATION–TRAJECTORY OPTIMIZATION SCHEME

In this section, the joint trajectory optimization and optimum power allocation of MD and UAV to minimize the outage probability is derived. This joint optimization problem is formulated as:

$$\min_{P,x,y,z} P_{out}, \tag{15a}$$

$$s.t.\ P_M + P_U \leq P_{max}, \tag{15b}$$

$$0 < P_M, 0 < P_U, 0 < P_{d2d} \tag{15c}$$

$$\gamma_{d2d_i} \geq T, \tag{15d}$$

$$d_{t,t-1} \leq v, x \forall t \in N, \tag{15e}$$

where P_{max} is the system budget power dedicated for the communication link between the MD and the BS. (15b) and (15c) are the power constraints that satisfy all the powers are positive and the sum of the MD and UAV powers are less than or equal to the budget power system P_{max}. The constrain (15d) is provided to guarantee good quality of service (QoS) at the D2D devices, where T is the minimum SINR required for any D2D receiving device. (15e) is the UAV mobility constraint, where $d_{t,t-1}$ is the flying distance of the UAV in time slot $t-1$. It is assumed that the flying distance of the UAV in one time slot cannot exceed v. Here, $v \ll D$.

To solve the optimization problem presented in (15), we decouple it into trajectory optimization and power allocation sub–problems. The two sub–problems are solved individually in an iterative manner. Then, the joint power allocation–trajectory optimization algorithm is presented.

A. POWER OPTIMIZATION

The objective is to minimize the outage probability expression given in (11) by optimizing the transmit powers P_M and P_U given a fixed trajectory for the UAV. Thus, problem (15) can be formulated as:

$$\min_{P} P_{out}, \tag{16a}$$

$$s.t.\ P_M + P_U \leq P_{max}, \tag{16b}$$

$$0 < P_M, 0 < P_U, 0 < P_{d2d} \tag{16c}$$

$$\gamma_{d2d_i} \geq T. \tag{16d}$$

The QoS is guaranteed when $\gamma_{d2d} = T$. Therefore, from (10), the power of the i_{th} D2D device that guarantee the QoS at the i_{th} D2D is expressed as:

$$P_{d2d} = \Big\{ \frac{T \Big[P_M ||h_{M,d2d_i}||^2 + P_U ||h_{U,d2d_i}||^2 + N_o \Big]}{||h_{d2d_{Tx_i}, d2d_{Rx_i}}||^2 - T \sum_{j=1, j\neq i}^{M} ||h_{d2d_{Tx_j}, d2d_{Rx_j}}||^2} \Big\}. \tag{17}$$

or equivalently:

$$P_{d2d} = \mu_1 P_M + \mu_2 P_U + \mu_3 N_o, \tag{18}$$

where

$$\mu_1 = \frac{T ||h_{M,d2d_i}||^2}{||h_{d2d_{Tx_i}, d2d_{Rx_i}}||^2 - T \sum_{j=1, j\neq i}^{M} ||h_{d2d_{Tx_j}, d2d_{Rx_j}}||^2}, \tag{20a}$$

$$\mu_2 = \frac{T||h_{U,d2d_i}||^2}{||h_{d2d_{Tx_i},d2d_{Rx_i}}||^2 - T\sum_{j=1,j\neq i}^{M}||h_{d2d_{Tx_j},d2d_{Rx_j}}||^2}, \tag{20b}$$

$$\mu_3 = \frac{T}{||h_{d2d_{Tx_i},d2d_{Rx_i}}||^2 - T\sum_{j=1,j\neq i}^{M}||h_{d2d_{Tx_j},d2d_{Rx_j}}||^2}. \tag{20c}$$

Then, by substituting (17) in (11) and by letting the power of the UAV $P_U = P_{max} - P_M$ from (16b), the outage probability of the link from the MD to the BS is given by:

$$P_{out} = 1 - exp(I), \tag{21}$$

where I is given by (19), as shown at the bottom of the page and A is given as:

$$A = \frac{-B_{th}(4\pi f)^2}{2C^2 G_U},$$

To minimize the outage probability given in (21), the exponential term must be maximized. The maximization of the second exponential term is performed by minimizing the power of the exponential, that is minimizing I with respect to P_M.

To obtain the power P_M that minimizes I, $\frac{\partial I}{\partial P_M}$ is obtained and equated to zero. After mathematical manipulation, P_M is obtained as the solution of the following quadratic equation:

$$\Delta {P_M}^2 + \Gamma P_M + \Phi = 0 \tag{22}$$

where

$$\Delta = A \times \Big[P_{max}\big[\mu_1 Z\sum_{i=1}^{M}||h_{d2d_i,BS}||^2 - \mu_2 Y\sum_{i=1}^{M}||h_{d2d_i,U}||^2\big] + N_o \big[\mu_3 Z\sum_{i=1}^{M}||h_{d2d_i,BS}||^2 + Z - \mu_3 Y\sum_{i=1}^{M}||h_{d2d_i,U}||^2\big] - XY\Big], \tag{23}$$

$$\Gamma = 2P_{max}AY\Big[\sum_{i=1}^{M}||h_{d2d_i,U}||^2\big[\mu_2 P_{max} + \mu_3 N_o\big] + X\Big], \tag{24}$$

$$\Phi = -{P_{max}}^2 AY\Big[\sum_{i=1}^{M}||h_{d2d_i,U}||^2\big[\mu_2 P_{max} + \mu_3 N_o\big] + X\Big]. \tag{25}$$

The solution of this quadratic equation is expressed as:

$$P_M^* = \frac{-\Gamma \pm \sqrt{\Gamma^2 - 4\Delta\Phi}}{2\Delta}. \tag{26}$$

From (16b), P_U^* is given as:

$$P_U^* = P_{max} - P_M^*, \tag{27}$$

where only positive power values are considered as constrained in (16c).

B. TRAJECTORY OPTIMIZATION

In this subsection, we minimize the total outage probability expression presented in (11) by optimizing the trajectory of the UAV given equal power allocation for the MD and the UAV. In other words, $P_M = P_U = \frac{P_{max}}{2}$. According to (17), the minimum power of any D2D transmitting device when $P_M = P_U = \frac{P_{max}}{2}$ is denoted as $P_{d2d_{eq}}$ and is given as:

$$P_{d2d_{eq}} = \frac{T\Big[0.5P_{max}||h_{M,d2d_i}||^2 + 0.5P_{max}||h_{U,d2d_i}||^2 + N_o\Big]}{||h_{d2d_{Tx_i},d2d_{Rx_i}}||^2 - T\sum_{j=1,j\neq i}^{M}||h_{d2d_{Tx_j},d2d_{Rx_j}}||^2}. \tag{28}$$

Consequently, problem (15) can be expressed as:

$$\sum_{t\in N}\min_{x,y,z} P_{out}, \tag{29a}$$

$$d_{t,t-1} \leq v, x \forall t \in N. \tag{29b}$$

Since problem (29a) is non–convex with x, y and z, to solve such a problem, we decouple it into $N-1$ sub–problems. Accordingly, we minimize the outage probability in different time slots serially. The sub–problem for a given time slot t can be expressed as:

$$\min_{x^t,y^t,z^t} P_{out}^t, \tag{30a}$$

$$d_{t,t-1} \leq v, x \forall t \in N. \tag{30b}$$

From (11), P_{out}^t can be expressed as:

$$P_{out} = 1 - \exp\Big\{-\frac{\beta_{th}(4\pi f)^2}{2C^2 G_U}\Big[C_a D_{M,U}^2 e^{k(f)D_{M,U}} + C_b D_{U,BS}^2 e^{k(f)D_{U,BS}}\Big]\Big\}, \tag{31}$$

where

$$C_a = \frac{P_{d2d}\sum_{i=1}^{M}||h_{d2d_i,U}||^2 + {\gamma_r}^2 P_{rr}||h_{rr}||^2 + N_o}{\frac{1}{2}G_M P_{max}}, \tag{32a}$$

$$C_b = \frac{P_{d2d}\sum_{i=1}^{M}||h_{d2d_i,BS}||^2 + N_o}{\frac{1}{2}G_U P_{max}}. \tag{32b}$$

$$I = \Big\{\frac{AY\sum_{i=1}^{M}||h_{d2d_i,U}||^2(\mu_1 P_M + \mu_2(P_{max} - P_M) + \mu_3 N_o) + AXY}{P_M} + \frac{AZ\sum_{i=1}^{M}||h_{d2d_i,BS}||^2(\mu_1 P_M + \mu_2(P_{max} - P_M) + \mu_3 N_o) + AZN_o}{P_{max} - P_M}\Big\} \tag{19}$$

Substituting by $D_{M,U}$ and $D_{U,BS}$ expressed in (1) and (2) in (31), the total outage probability can be expressed as:

$$P_{out} = 1 - \exp\left\{ - \frac{\beta_{th}(4\pi f)^2}{2C^2 G_U}\left[C_a((x_t - D)^2 + y_t^2 + z_t^2)\right.\right.$$
$$e^{k(f)\sqrt{((x_t-D)^2+y_t^2+z_t^2}} + C_b(x_t^2 + y_t^2 + (z_t - H)^2)$$
$$\left.\left. e^{k(f)\sqrt{(x_t^2+y_t^2+(z_t-H)^2)}}\right]\right\}. \quad (33)$$

Let:

$$f(x, y, z) = C_a(x_t - D)^2 + y_t^2 + z_t^2)e^{k(f)\sqrt{(x_t-D)^2+y_t^2+z_t^2}}$$
$$+C_b(x_t^2 + y_t^2 + (z_t - H)^2 e^{k(f)\sqrt{(x_t^2+y_t^2+(z_t-H)^2)}}. \quad (34)$$

Since $f(x, y, x)$ is monotonically increasing, minimizing P_{out} is equivalent to minimizing $f(x, y, z)$ [35]. Thus, problem (15) can be rewritten as:

$$\min_{x,y,z} f(x, y, z), \quad (35a)$$
$$d_{t,t-1} \leq v.x \forall t \in N. \quad (35b)$$

Since problem (35) is convex and it satisfies slater's condition [36], the gap between the optimal value of problem (35) and that of its dual problem is zero. Consequently, this problem can be solved by getting the solution of the dual problem [36].

Let λ be the Lagrangian multiplier that corresponds to the moving distance constraint given in (35b). Therefore, the Lagrangian of problem (35) is:

$$L(x_t, y_t, z_t, \lambda) = f(x_t, y_t, z_t) + \lambda(d_{t,t-1} - v), \quad (36)$$

and the dual objective is:

$$g(\lambda) = \inf_{x_t, y_t, z_t} L(x_t, y_t, z_t, \lambda). \quad (37)$$

Thus, the dual problem of (35) can be expressed as:

$$\max_{\lambda} g(\lambda), \quad (38a)$$
$$s.t.\ \lambda \geq 0. \quad (38b)$$

Since $g(\lambda)$ is not differenciable, sub–gradient method is deployed to pick dual problem (38). In fact, the sub–gradient method is implemented to find the feasible solution in the chosen sub– gradient direction. By letting λ^w represents the w^{th} iteration, it is proven that the sub– gradient of the dual function $g(\lambda)$ at λ^w is expressed as:

$$q^w = \sqrt{(x_t^w - x_{t-1})^2 + (y_t^w - y_{t-1})^2 + (z_t^w - z_{t-1})^2} - v, \quad (39)$$

where (x_t^w, y_t^w, z_t^w) minimizes the Lagrangian $L(x_t, x_t, x_t, \lambda^w)$ [37]. q^w is selected as the sub–gradient. Moreover, the step size is selected as:

$$\alpha^w = \frac{a}{b + w}, \quad (40)$$

where $a > 0$ and $b \geq 0$. Consequently, λ is updated in each iteration according to the following rule:

$$\lambda^{w+1} = [\lambda^w + \alpha^w q^w]^+, \quad (41)$$

Algorithm 1 Trajectory Optimization Algorithm

Input: The transmit power P.
Output: The trajectory J.
for $t = 2 : N$ **do**
  Initialize: $w = 0, \lambda^0 = 1$
  while $| g(\lambda^w) - g(\lambda^{w-1}) | > \epsilon_2$ **do**
    Use Karush–Kuhn–conditions to obtain the optimal trajectory (x_w^t, y_w^t, z_w^t).
    Update λ *according to (41);*
    $w = w + 1$;

where the notation $[X]^+$ means $max(X, 0)$. In fact, λ represents the price factor for the moving distance constraint. Furthermore, it surely increases in case the moving distance constraint is contradicted. Hence, the sub–gradient method tells that λ increases if $d_{t,t-1} > v$ and decreases otherwise. The iteration process comes to an end when $|g(\lambda^{w+1}) - g(\lambda^w)| < \epsilon_2$ is satisfied, where ϵ_2 is the error tolerance for the trajectory optimization algorithm.

Referring to Karush–Kuhn–Tucker conditions, the optimal trajectory is obtained by getting $\Delta f(x_t, y_t, z_t) = 0$. Then, the obtained trajectory is substituted into (41) in order to calculate λ^{w+1}. In each iteration, the optimum trajectory $J_t^{opt} = (x_t^{opt}, y_t^{opt}, z_t^{opt})$ is obtained numerically, where it is within the moving ability of the UAV in time slot $t - 1$. After that, the UAV moves to J_t^{opt} in time slot $t - 1$. Algorithm 1 summarizes the procedure for solving the trajectory design sub–problem.

C. JOINT POWER ALLOCATION–TRAJECTORY OPTIMIZATION ALGORITHM

Let:

$$P_{t,out}^{(k)} = \sum_{t \in N} (P_{out}^t)^{(k)}, \quad (42)$$

where $P_{t,out}^{(k)}$ is the total outage probability in the k^{th} iteration. Then, the joint power allocation and trajectory optimization problem is summarized in Algorithm 2, where ϵ_1 is the predetermined error tolerance for the joint power allocation trajectory optimization algorithm. Both Algorithm 1 and Algorithm 2 are considered as convex quadratic optimization (CQO) problems, where both interior-point algorithms are based on potential reduction approach (ϵ) with iteration bound $\mathcal{O}(n \log \frac{n}{\epsilon})$ in the worst case [38].

VI. ACHIEVABLE RATE MAXIMIZATION OPTIMIZATION PROBLEM

In this section, the objective is to obtain the transmit powers P_M and P_U that maximize the achievable data rate.

Let $R_{M,U}$ and $R_{U,BS}$ be the achievable data rates at the UAV (DF–relay) and the BS, respectively, where:

$$R_{M,U} = Wlog_2(1 + \gamma_U), \quad (43a)$$
$$R_{U,BS} = Wlog_2(1 + \gamma_{BS}), \quad (43b)$$

Algorithm 2 Joint Trajectory Optimization and Power Allocation Algorithm

Initialize: $k = 1, x^t = x_o, y^t = y_o, z^t = z_o, \forall t \in N$

while $\frac{|P_{t,out}^{(k)} - P_{t,out}^{(k-1)}|}{P_{t,out}^{(k-1)}} > \epsilon_1$ **do**

Given the trajectory of the UAV, solve the power allocation sub–problem (16).

Given the power allocation, solve the trajectory optimization problem (29a).

$k = k + 1;$

where W is the available bandwidth in THz band, γ_U and γ_{BS} are given in (7) and (8), respectively. The data rate from source to destination using DF–FD relaying is given by $min(R_{M,U}, R_{U,BS})$ [39]. Then, the optimization problem can be formulated as:

$$\max_{P_M, P_U} \min(Wlog_2(1+\gamma_U), W\ log_2(1+\gamma_{BS})), \tag{44a}$$
$$s.t.\ 0 < P_M, 0 < P_U, 0 < P_{d2d} \tag{44b}$$
$$xP_M + P_U \leq P_{max}, \tag{44c}$$
$$\gamma_{d2d_i} \geq T. \tag{44d}$$

In order to satisfy the minimum required SINR at any D2D receiving device represented in (44d), γ_{d2d} should be at least equal to T. Then, by substituting the minimum P_{d2d} expressed in (18) in (7) and (8), γ_U and γ_{BS} can be expressed as:

$$\gamma_U = \frac{C_1 P_M}{C_2 P_M + C_3}, \tag{45a}$$
$$\gamma_{BS} = \frac{C_4 P_U}{C_5 P_M + C_6}, \tag{45b}$$

where

$$C_1 = ||h_{M,U}||^2, \tag{46a}$$
$$C_2 = (\mu_1 - \mu_2) \sum_{i=1}^{M} ||h_{d2d_i,U}||^2, \tag{46b}$$
$$C_3 = \mu_2 \sum_{i=1}^{M} ||h_{d2d_i,U}||^2 P_{max} + \mu_3 N_o \sum_{i=1}^{M} ||h_{d2d_i,U}||^2 + {\gamma_r}^2 ||h_{rr}||^2 P_{rr} + No, \tag{46c}$$
$$C_4 = ||h_{U,BS}||^2, \tag{46d}$$
$$C_5 = (\mu_1 - \mu_2) \sum_{i=1}^{M} ||h_{d2d_i,BS}||^2, \tag{46e}$$
$$C_6 = \mu_2 \sum_{i=1}^{M} ||h_{d2d_i,BS}||^2 P_{max} + \mu_3 N_o \sum_{i=1}^{M} ||h_{d2d_i,BS}||^2 + No. \tag{46f}$$

Now, problem (44) can be reduced to:

$$\max_{P_M, P_U} \min(Wlog_2(1+\gamma_U), W\ log_2(1+\gamma_{BS})), \tag{47a}$$
$$s.t.\ 0 < P_M \leq P_{M_{max}}, 0 < P_U \leq P_{U_{max}} \tag{47b}$$
$$xP_M + P_U \leq P_{max}, \tag{47c}$$

where $P_{M_{max}}$ and $P_{U_{max}}$ are the maximum values of P_M and P_U, respectively. Because the function $\log_2(.)$ is monotonically increasing and since γ_U and γ_{BS} are directly proportional to $R_{M,U}$ and $R_{U,BS}$ respectively, this optimization problem can be reformulated as:

$$\max_{P_M, P_U} \min(\gamma_U, \gamma_{BS}), \tag{48a}$$
$$s.t.\ 0 < P_M \leq P_{M_{max}}, 0 < P_U \leq P_{U_{max}} \tag{48b}$$
$$xP_M + P_U \leq P_{max}. \tag{48c}$$

From (48a), it is obvious that the achieved end–to–end SINR of the system depends on the minimum value of the two hops namely γ_U and γ_{BS}. In order to maximize the end–to–end SINR, the transmit powers of the MD, P_M and the UAV, P_U should be adaptively adjusted to guarantee that $\gamma_U = \gamma_{BS}$. Hence, by equating (45a) and (45b), the following holds:

$$(C_1C_5 + C_2C_4)P_M^2 + (C_1C_6 - C_2C_4P_{max} + C_3C_4)P_M - C_3C_4P_{max} = 0. \tag{49}$$

Let:

$$k_1 = C_1C_5 + C_2C_4, \tag{50a}$$
$$k_2 = C_1C_6 - C_2C_4P_{max} + C_3C_4, \tag{50b}$$
$$k_3 = -C_3C_4P_{max}, \tag{50c}$$

where P_U is substituted by $P_{max} - P_M$ as constrained in (48c).

Therefore, the optimization problem in (48) can be expressed as:

$$k_1P_M^2 + k_2P_M + k_3 = 0, \tag{51a}$$
$$s.t.\ x0 < P_M < P_{M_{max}}. \tag{51b}$$

From (51), the optimum MD power that maximizes the achieved rate from MD to BS is given as:

$$P_{M_{opt}}^* = \frac{-k_2 \pm \sqrt{k_2^2 - 4k_1k_3}}{2k_1}, \tag{52}$$

where only the positive power value is accepted. The optimum MD power that maximizes the rate from the MD to the BS can be expressed as:

$$P_M^* = \begin{cases} P_{M_{max}} & if\ P_M^* > P_{M_{max}} \\ P_{M_{opt}}^* & if\ P_{max} - P_{U_{max}} \leq P_M^* \leq P_{M_{max}} \\ P_{max} - P_{U_{max}} & if\ P_M^* < P_{max} - P_{U_{max}} \end{cases} \tag{53}$$

Then, the optimum power of the UAV can be calculated as $P_U^* = P_{max} - P_M^*$. From (53), it is noted that P_M^* and consequently P_U^* are constants in the two extreme cases: $P_M^* > P_{M_{max}}$ and $P_M^* < P_{max} - P_{U_{max}}$. The more general case is $P_{max} - P_{U_{max}} \leq P_M^* \leq P_{M_{max}}$ which depends on the distances between the MD and the UAV, $D_{M,U}$ and the distance from the UAV to the BS, $D_{U,BS}$.

TABLE 1. Simulation Parameters.

Parameter	Description	Value
f	Operating Frequency	1 THz
$k(f)$	Absorption Coefficient	0.1
P_{max}	Power Budget	0 dB
N_o	Noise Variance	-50 dBm
B_{th}	Threshold of γ_U and γ_{BS}	-80 dB
H	Height of BS	15 m
G_{d2d}	Gain of the D2D device	20 dB
$P_{M_{max}}$	Maximum MD Power	0.8 W
$P_{U_{max}}$	Maximum UAV Power	0.8 W

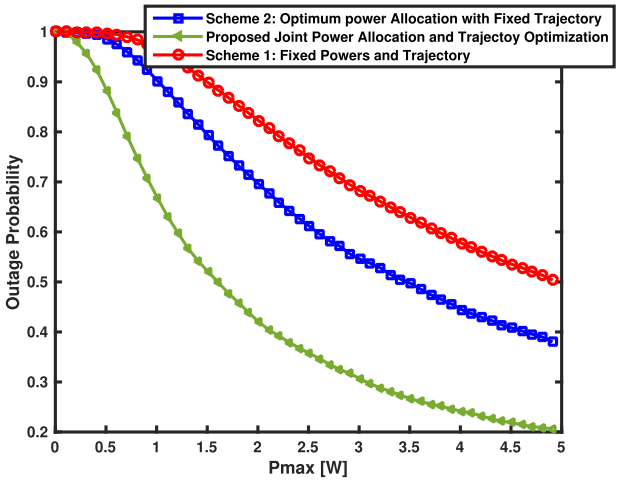

FIGURE 3. Outage Probability achieved through the fixed power and trajectory, optimum power allocation with fixed trajectory and joint power allocation and trajectory optimization schemes vs. P_{max} for $x_o = 60$ m, $y_o = 0$, $z_o = 22.5$ m.

VII. NUMERICAL RESULTS

In this section, the joint power allocation and trajectory optimization scheme that minimize the total outage probability at the BS as well as the rate maximization optimization problem are evaluated. The performance of the schemes is compared to the fixed power and trajectory scheme that blindly divides the system power budget between the MD and the BS equally and assumes a fixed position of the UAV. The simulations are performed at 1 THz, which is one of the transmission windows at THz frequency range presented in [40]. The values of the simulation parameters are summarized in Table 1.

A. PROPOSED JOINT POWER ALLOCATION AND TRAJECTORY OPTIMIZATION SCHEME

In this subsection, the proposed power allocation with trajectory optimization scheme is evaluated to obtain the optimum powers and optimum trajectory that minimize the outage probability expressed in (11). Two schemes are included for comparison purpose. The first scheme is the fixed powers and trajectory scheme; we call it "Scheme 1". The second one is the optimum power allocation with fixed trajectory; we call it "Scheme 2".

Fig. 3 shows the outage probability for the proposed joint power allocation and trajectory optimization versus the system power budget P_{max}. The figure shows that the outage probability decreases with increasing P_{max}. Moreover, the proposed joint power allocation trajectory optimization scheme achieves the lowest outage probability. This is due to the adaptability of the proposed scheme that assigns powers according to the instance UAV position and assigns the optimized trajectory according to the powers of the MD and the UAV. The figure also shows that the proposed joint power allocation and trajectory optimization scheme outperforms Scheme 2. This is because Scheme 2 optimizes only the powers of the MD and the UAV without adapting the UAV position accordingly. It is also shown that the proposed scheme outperforms Scheme 1. This is because the UAV has a fixed position and the system power budget is blindly divided equally between the MD and the UAV.

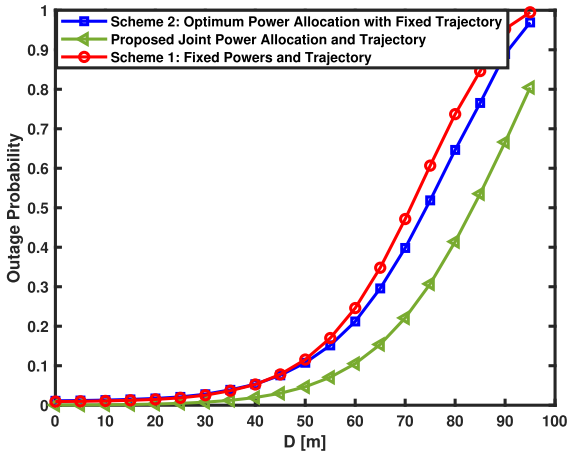

FIGURE 4. Outage Probability achieved through the fixed power and trajectory, optimum power allocation with fixed trajectory and joint power allocation and trajectory optimization schemes vs. D for $x_o = 60$ m, $y_o = 0$, $z_o = 22.5$ m.

Fig. 4 shows the outage probability for the proposed joint power allocation and trajectory optimization versus the distance D between the MD and the BS. Again, the two mentioned schemes are included for comparison purposes. As the figure depicts, increasing the distance between the MD and the UAV results in an increase in the outage probability. This is due to the higher pathloss that the propagating signal encounters at a longer travelling distance which is one of the challenges of THz communications. This problem can be solved using MIMO system which increases the transmit power significantly. Furthermore, the lowest outage probability is achieved by the proposed joint power allocation and trajectory scheme followed by Scheme 2 and then Scheme 1.

Fig. 5 shows the outage probability for the same three schemes versus the BS height H. As before, the lowest outage probability is achieved by the joint power allocation and trajectory optimization scheme. It is noticed that the outage probability for the proposed scheme decreases whenever H increases till $H \approx 22.5m$ which is equal to the height of the UAV. This height corresponds to a shorter distance between the UAV and the BS, $D_{U,BS}$. When H increases forward, $D_{U,BS}$ increases, which leads to an

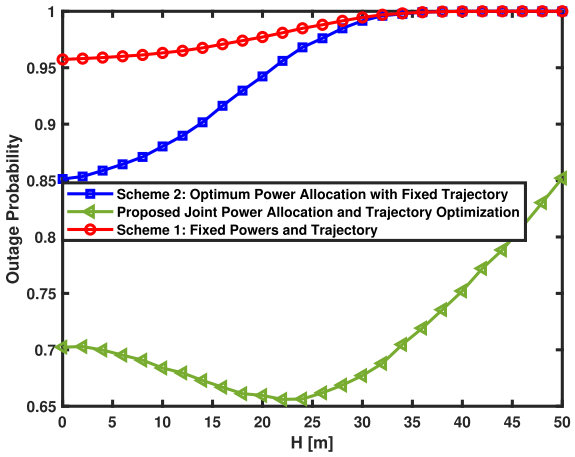

FIGURE 5. Outage Probability achieved through the fixed power and trajectory, optimum power allocation with fixed trajectory and joint power allocation and trajectory optimization schemes vs. H for $x_o = 60$ m, $y_o = 0$, $z_o = 22.5$ m.

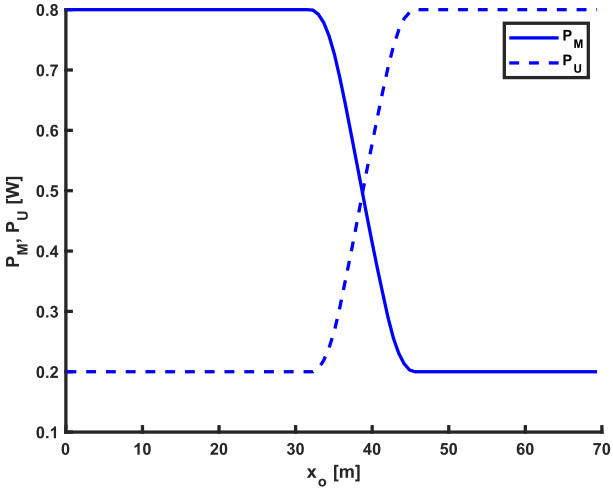

FIGURE 6. P_M and P_U at different locations of the UAV at $D = 70$ m.

increase in the outage probability due to an increase in the distance between the UAV and the BS.

B. RATE MAXIMIZATION SCHEME

In this subsection, the rate maximization scheme introduced is evaluated.

Fig. 6 shows the optimum powers P_M and P_U that maximize the achievable rate at the BS versus the horizontal distance x_o between the BS and the UAV. When x_o is zero, which means that the UAV is exactly above the BS, the MD is assigned the maximum MD power value $P_{M_{max}}$ and P_U is assigned a lower power; which is the remaining power budget $P_{max} - P_{M_{max}}$. These power values are retained until $x_o \approx 30$ m. When $x_o > 30$ m, P_M gradually decreases since the link between the MD and the UAV gets better. However, P_U increases since the link between the UAV and the BS gets worse. Similarly, whenever the UAV is exactly above the MD (i.e. $x_o = 70$ m), the maximum UAV power value

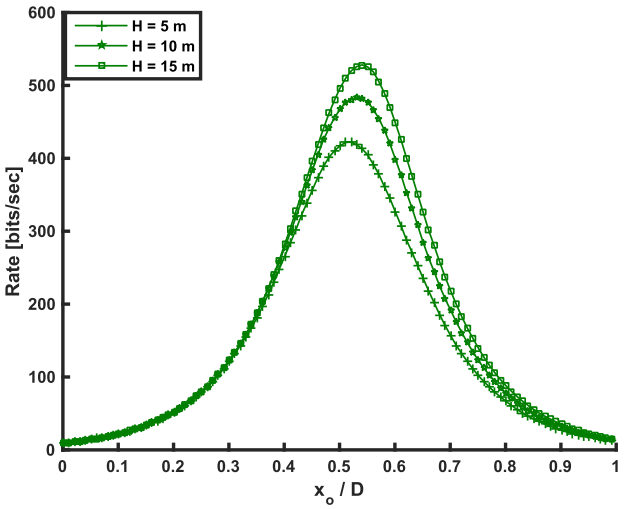

FIGURE 7. Achieved Rate versus $\frac{x_o}{D}$ for different T values at $D = 70$ m.

$P_{U_{max}}$ is assigned to P_U since it suffers from very high fading and distortion due to the long distance travelled. It can be mentioned that at $x_o = 70$ m, there is no need to invest a lot of power in the link between the MD and the UAV. This is because of the optimum power allocation scheme that adapts with the given scenario instead of assigning fixed powers to the MD and the UAV. It is worth mentioning that the summation of P_M and P_U at any given scenario is P_{max}.

Fig. 7 shows the achieved rate for different BS heights H. It is noted that increasing the BS height results in increasing the rate achieved. From the system model represented in Fig. 1, increasing the BS height H above zero shortens the distance between the BS and the UAV. This in return leads to decreasing the distance between the UAV and the BS denoted as $D_{U,BS}$. Because the travelled distance is inversely proportional to the achieved rate, the rate increases whenever H decreases. In addition, it is clear that the rate achieved is maximum whenever the UAV is placed in the middle between the MD and the BS (ex: $\frac{x_o}{D} = 0.5$). This is because at this certain UAV placement scenario, the achievable rates values at the UAV and the BS are very close.

Fig. 8 shows the achieved rate obtained using the derived optimum power allocation scheme compared with the achievable rate obtained using fixed power allocation scheme versus the normalized distance x_o/D. The figure plotted for different values of the SINR thresholds T of the D2D devices. The figure shows that the proposed optimum power allocation scheme outperforms the fixed power allocation scheme for all values of T. The figure also shows that, as T increases, the achieved rate decreases. This is because increasing T leads to an increase in the assigned power for the D2D device P_{d2d} which in turn increases the interference caused by D2D devices at the UAV and the BS receiving antennas. Consequently, higher rate is achieved at small values of T.

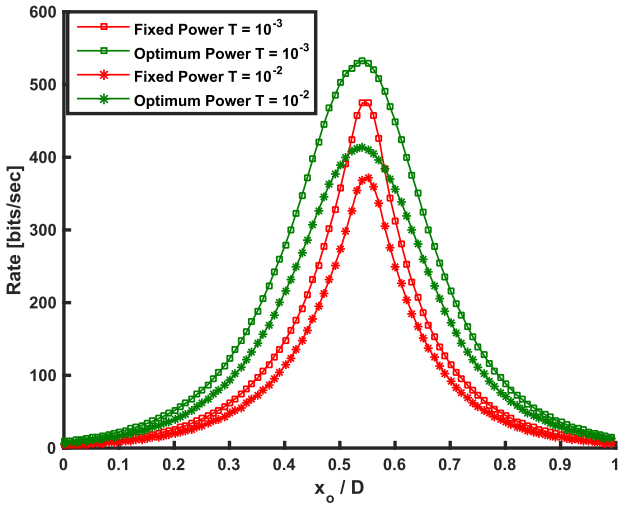

FIGURE 8. Achieved Rate versus $\frac{x_o}{D}$ for different T values at $D = 70$ m.

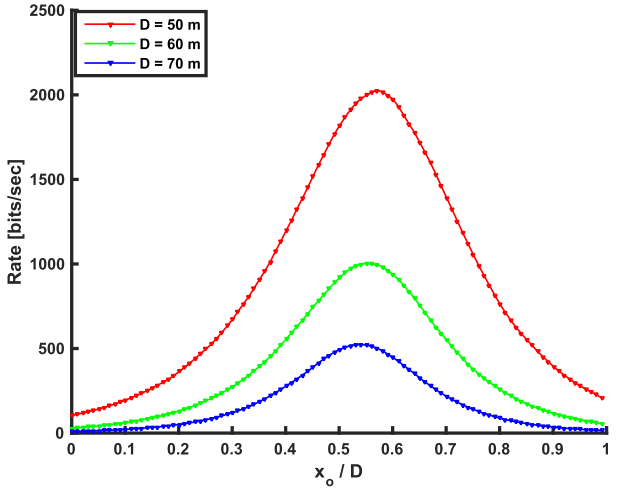

FIGURE 9. Achieved Rate versus $\frac{x_o}{D}$ for different at $D = 50$, 60 and 70 m.

Fig. 9 shows the achieved rate versus $\frac{x_o}{D}$ at different distances between the MD and the BS D at BS height $H = 15$ m and minimum SINR threshold of D2D $T = 10^{-3}$. As expected, whenever the distance between the MD and the BS increases, the achieved rates decreases drastically due to the substantial path loss the signal experiences. Consequently, the rate decreases whenever the distance between the MD and the BS increases due to the inverse proportionality between them.

Fig. 10 shows the outage probability when using the optimum powers allocation that minimize the achievable outage probability as presented in Algorithm 1 as well as the achieved outage probability when utilizing the powers allocation that maximize the achievable rate, at a fixed trajectory. It is noted that the outage probability achieved due to the optimum powers that minimize the outage probability

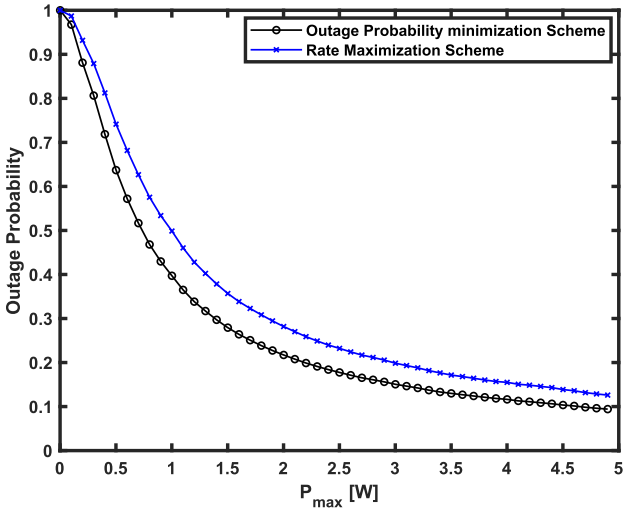

FIGURE 10. Achieved Outage Probability versus P_{max} when using Optimum Powers for Outage Probability Minimization Algorithm and Optimum Powers for the Rate Maximization Algorithm, respectively.

(Algorithm 1) is better than that achieved when using the optimum powers that maximize the achievable rate.

VIII. CONCLUSION

In this paper, a joint power allocation and trajectory optimization scheme that minimizes the outage probability of the link between the MD and the BS in THz channel is proposed. Moreover, a rate maximization scheme is proposed in order to extend the coverage of the BS, where the optimum powers of the MD and the BS that maximize the achievable rate at the BS are obtained. The UAV is deployed as a DF–FD relay in order to extend the coverage of the BS. Numerical results show that the total outage probability achieved by the joint power allocation and trajectory optimization scheme is much better than the total outage probability achieved in the case of fixed power and trajectory scheme. Moreover, the achieved proposed rate maximization scheme that optimizes the MD and UAV transmitted powers is found superior to that fixed power allocation scheme achieved rate that assigns equal fixed powers to the MD and the UAV. For future work, MIMO system could be implemented and antenna arrays are utilized to increase the transmit powers effectively and achieve a higher directivity in our proposed UAV–relaying system.

REFERENCES

[1] H. Sarieddeen, M.-S. Alouini, and T. Y. Al-Naffouri, "An overview of signal processing techniques for terahertz communications," *Proc. IEEE*, vol. 109, no. 10, pp. 1628–1665, Oct. 2021.

[2] Q. Ye, J. Cho, J. Jeon, S. Abu-Surra, K. Bae, and J. C. Zhang, "Fractionally spaced equalizer for next generation terahertz wireless communication systems," in *Proc. IEEE Int. Conf. Commun. Workshops (ICC Workshops)*, Jun. 2021, pp. 1–7.

[3] M. Polese, J. M. Jornet, T. Melodia, and M. Zorzi, "Toward end-to-end, full-stack 6G terahertz networks," *IEEE Commun. Mag.*, vol. 58, no. 11, pp. 48–54, Nov. 2020.

[4] Y. Corre, G. Gougeon, J.-B. Doré, S. Bicaïs, B. Miscopein, E. Faussurier, M. Saad, J. Palicot, and F. Bader, "Sub-THz spectrum as enabler for 6G wireless communications up to 1 Tbit/s," in *Proc. 6G Wireless Summit*, 2019.

[5] C. Lin and G. Y. Li, "Indoor terahertz communications: How many antenna arrays are needed?" *IEEE Trans. Wireless Commun.*, vol. 14, no. 6, pp. 3097–3107, Jun. 2015.

[6] H. Elayan, R. M. Shubair, J. M. Jornet, and P. Johari, "Terahertz channel model and link budget analysis for intrabody nanoscale communication," *IEEE Trans. Nanobiosci.*, vol. 16, no. 6, pp. 491–503, Sep. 2017.

[7] Z. Chen, X. Ma, B. Zhang, Y. Zhang, Z. Niu, N. Kuang, W. Chen, L. Li, and S. Li, "A survey on terahertz communications," *China Commun.*, vol. 16, no. 2, pp. 1–35, 2019.

[8] M. Burla, C. Hoessbacher, W. Heni, C. Haffner, Y. Fedoryshyn, D. Werner, T. Watanabe, H. Massler, D. L. Elder, L. R. Dalton, and J. Leuthold, "500 GHz plasmonic Mach–Zehnder modulator enabling sub-THz microwave photonics," *APL Photon.*, vol. 4, no. 5, May 2019, Art. no. 056106.

[9] O. Elkharbotly, E. Maher, A. El-Mahdy, and F. Dressler, "Optimal power allocation in cooperative MIMO-NOMA with FD/HD relaying in THz communications," in *Proc. 9th IFIP Int. Conf. Perform. Eval. Modeling Wireless Netw. (PEMWN)*, Dec. 2020.

[10] A. Saeed, O. Gurbuz, and M. A. Akkas, "Terahertz communications at various atmospheric altitudes," *Phys. Commun.*, vol. 41, Aug. 2020, Art. no. 101113.

[11] O. D. Oyeleke, S. Thomas, O. Idowu-Bismark, P. Nzerem, and I. Muhammad, "Absorption, diffraction and free space path losses modeling for the terahertz band," *Int. J. Eng. Manuf.*, vol. 10, p. 54, Feb. 2020.

[12] N. Elburki, S. Ben Amor, and S. Affes, "Evaluation of path-loss models for THz propagation in indoor environments," in *Proc. IEEE Can. Conf. Electr. Comput. Eng. (CCECE)*, Aug. 2020, pp. 1–5.

[13] H. Elayan, O. Amin, B. Shihada, R. M. Shubair, and M.-S. Alouini, "Terahertz band: The last piece of RF spectrum puzzle for communication systems," *IEEE Open J. Commun. Soc.*, vol. 1, pp. 1–32, 2019.

[14] W. Hedhly, "Resource allocation in future terahertz networks," Ph.D. dissertation, 2019.

[15] K. Li, W. Ni, and F. Dressler, "Continuous maneuver control and data capture scheduling of autonomous drone in wireless sensor networks," *IEEE Trans. Mobile Comput.*, early access, Jan. 5, 2021, doi: 10.1109/TMC.2021.3049178.

[16] A. Fotouhi, H. Qiang, M. Ding, M. Hassan, L. G. Giordano, A. Garcia-Rodriguez, and J. Yuan, "Survey on UAV cellular communications: Practical aspects, standardization advancements, regulation, and security challenges," *IEEE Commun. Surveys Tuts.*, vol. 21, no. 4, pp. 3417–3442, 4th Quart., 2019.

[17] Z. Xiao, L. Zhu, and X.-G. Xia, "UAV communications with millimeter-wave beamforming: Potentials, scenarios, and challenges," *China Commun.*, vol. 17, no. 9, pp. 147–166, Sep. 2020.

[18] L. Zhu, J. Zhang, Z. Xiao, X. Cao, D. O. Wu, and X.-G. Xia, "3-D beamforming for flexible coverage in millimeter-wave UAV communications," *IEEE Wireless Commun. Lett.*, vol. 8, no. 3, pp. 837–840, Jun. 2019.

[19] H. Wang, J. Wang, G. Ding, J. Chen, Y. Li, and Z. Han, "Spectrum sharing planning for full-duplex UAV relaying systems with underlaid D2D communications," *IEEE J. Sel. Areas Commun.*, vol. 36, no. 9, pp. 1986–1999, Sep. 2018.

[20] Y. Pan, K. Wang, C. Pan, H. Zhu, and J. Wang, "UAV-assisted and intelligent reflecting surfaces-supported terahertz communications," *IEEE Wireless Commun. Lett.*, vol. 10, no. 6, pp. 1256–1260, Jun. 2021.

[21] S. Zhang, J. Liu, H. Guo, M. Qi, and N. Kato, "Envisioning device-to-device communications in 6G," *IEEE Netw.*, vol. 34, no. 3, pp. 86–91, Jun. 2020.

[22] N. A. Abbasi, J. Gomez-Ponce, R. Kondaveti, S. M. Shaikbepari, S. Rao, S. Abu-Surra, G. Xu, C. Zhang, and A. F. Molisch, "Thz band channel measurements and statistical modeling for urban D2D environments," 2021, *arXiv:2109.13693*.

[23] N. A. Tultul, S. S. Hossain, and S. Farha, "Device-to-device (D2D) communication in terahertz (THz) frequency band," Ph.D. dissertation, Brac Univ., Dhaka, Bangladesh, 2018.

[24] N. A. Tultul, S. Farha, S. S. Hossain, M. A. Hossain, and S. R. Sabuj, "Device-to-device communication in terahertz frequency band: Enhancement of energy efficiency," in *Proc. IEEE REGION Conf. (TENCON)*, Nov. 2020, pp. 117–122.

[25] E. Turgut and M. C. Gursoy, "Outage probability analysis in D2D-enabled mmWave cellular networks with clustered users," in *Proc. IEEE 88th Veh. Technol. Conf. (VTC-Fall)*, Aug. 2018, pp. 1–5.

[26] L. Zhu, J. Zhang, Z. Xiao, X. Cao, X.-G. Xia, and R. Schober, "Millimeter-wave full-duplex UAV relay: Joint positioning, beamforming, and power control," *IEEE J. Sel. Areas Commun.*, vol. 38, no. 9, pp. 2057–2073, Sep. 2020.

[27] H. Sarieddeen, M.-S. Alouini, and T. Y. Al-Naffouri, "An overview of signal processing techniques for terahertz communications," May 2020, *arXiv:2005.13176*.

[28] R. Mendrzik, D. Cabric, and G. Bauch, "Error bounds for terahertz MIMO positioning of swarm UAVs for distributed sensing," in *Proc. IEEE Int. Conf. Commun. Workshops (ICC Workshops)*, May 2018, pp. 1–6.

[29] Z. Guan and T. Kulkarni, "On the effects of mobility uncertainties on wireless communications between flying drones in the mmWave/THz bands," in *Proc. IEEE Conf. Comput. Commun. Workshops (INFOCOM WKSHPS)*, Apr. 2019, pp. 768–773.

[30] S. Farrag, E. Maher, A. El-Mahdy, and F. Dressler, "Outage probability analysis of UAV assisted mobile communications in THz channel," in *Proc. 16th Annu. Conf. Wireless On-Demand Netw. Syst. Services Conf. (WONS)*, Mar. 2021.

[31] H. Zhang, H. Zhang, W. Liu, K. Long, J. Dong, and V. C. M. Leung, "Energy efficient user clustering, hybrid precoding and power optimization in terahertz MIMO-NOMA systems," *IEEE J. Sel. Areas Commun.*, vol. 38, no. 9, pp. 2074–2085, Sep. 2020.

[32] A.-A.-A. Boulogeorgos, E. N. Papasotiriou, and A. Alexiou, "A distance and bandwidth dependent adaptive modulation scheme for THz communications," in *Proc. IEEE 19th Int. Workshop Signal Process. Adv. Wireless Commun. (SPAWC)*, Jun. 2018, pp. 1–5.

[33] L. Xu, M. Chen, M. Chen, Z. Yang, C. Chaccour, W. Saad, and C. S. Hong, "Joint location, bandwidth and power optimization for THz-enabled UAV communications," *IEEE Commun. Lett.*, vol. 25, no. 6, pp. 1984–1988, Jun. 2021.

[34] J. M. Jornet and I. F. Akyildiz, "Channel modeling and capacity analysis for electromagnetic wireless nanonetworks in the terahertz band," *IEEE Trans. Wireless Commun.*, vol. 10, no. 10, pp. 3211–3221, Oct. 2011.

[35] S. Zeng, H. Zhang, K. Bian, and L. Song, "UAV relaying: Power allocation and trajectory optimization using decode-and-forward protocol," in *Proc. IEEE Int. Conf. Commun. Workshops (ICC Workshops)*, May 2018, pp. 1–6.

[36] S. Boyd, S. P. Boyd, and L. Vandenberghe, *Convex Optimization*. Cambridge, U.K.: Cambridge Univ. Press, 2004.

[37] D. Bertsekas, "Mathematical programming for data mining: Formulations and challenges," *INFORMS J. Comput.*, vol. 11, pp. 217–238, Aug. 1999.

[38] J. Nie and Y. Yuan, "A potential reduction algorithm for an extended SDP problem," *Sci. China A, Math.*, vol. 43, no. 1, pp. 35–46, Jan. 2000.

[39] F. Benkhelifa, A. S. Salem, and M.-S. Alouini, "Rate maximization in MIMO decode-and-forward communications with an EH relay and possibly imperfect CSI," *IEEE Trans. Commun.*, vol. 64, no. 11, pp. 4534–4549, Nov. 2016.

[40] C. Han and I. F. Akyildiz, "Distance-aware multi-carrier (DAMC) modulation in terahertz band communication," in *Proc. IEEE Int. Conf. Commun. (ICC)*, Jun. 2014, pp. 5461–5467.